551.521.31 ; 551.583

TOTAL SOLAR IRRADIANCE (TSI) AND TERRESTRIAL CLIMATE

1. The sun emits a wide variety of radiations, originating in different parts (photosphere, chromosphere, chromosphere-corona transition region, corona) of the solar atmosphere. Solar ultraviolet (UV) irradiance (115-420 nm, 1150-4200 Å) originates mostly in the solar photosphere and chromosphere and, when absorbed in the earth's atmosphere, plays a dominant role in the temperature distribution, photochemistry, and overall momentum balance in the stratosphere, mesosphere, and lower thermosphere. The solar EUV flux, particularly below 130 nm (1300 Å) originates in the chromosphere, the chromosphere-corona transition region, and the solar corona (Donnelly *et al*., 1986) and is the primary cause of ion production in the ionosphere and contributes to the heating of the thermosphere. From sunspot minimum to sunspot maximum, the EUV increases by almost a factor of 2. However, the proportion of UV-EUV in the total solar irradiance (TSI) is rather small, only a few percent. The bulk of solar energy impinging on earth is in the visible and infrared region and it is mainly the TSI that supplies energy to lower terrestrial atmosphere. An interesting question is whether climatic changes are directly related to changes in TSI. Recent observations show that TSI changes are only ~0.1 %, in phase with sunspot cycle (Reid, 1999). On the other hand, climatic variability in some regions amounts to several percent, even on a year-to-year basis. Thus, some other factors must be responsible for climatic variability An important fact needs to be taken into consideration, namely, that the earth reflects a considerable amount of energy back to the outer space, more so from white clouds and snow. Thus, the energy budget should take into consideration not only the TSI input but also the losses due to reflections. It is difficult to estimate or to measure the reflected energy from various types of landmasses, sea surfaces, clouds etc. Low annual mean OLR values (< 200 Wm^{-2}) associated with deep atmospheric convection are found over the equatorial land masses, Amazon basin, and in the western equatorial Pacific. OLR < 200 Wm^{-2} are also associated with the cold temperatures of the Himalayas. High annual mean OLR values (> 280 Wm^{-2}) are observed over the

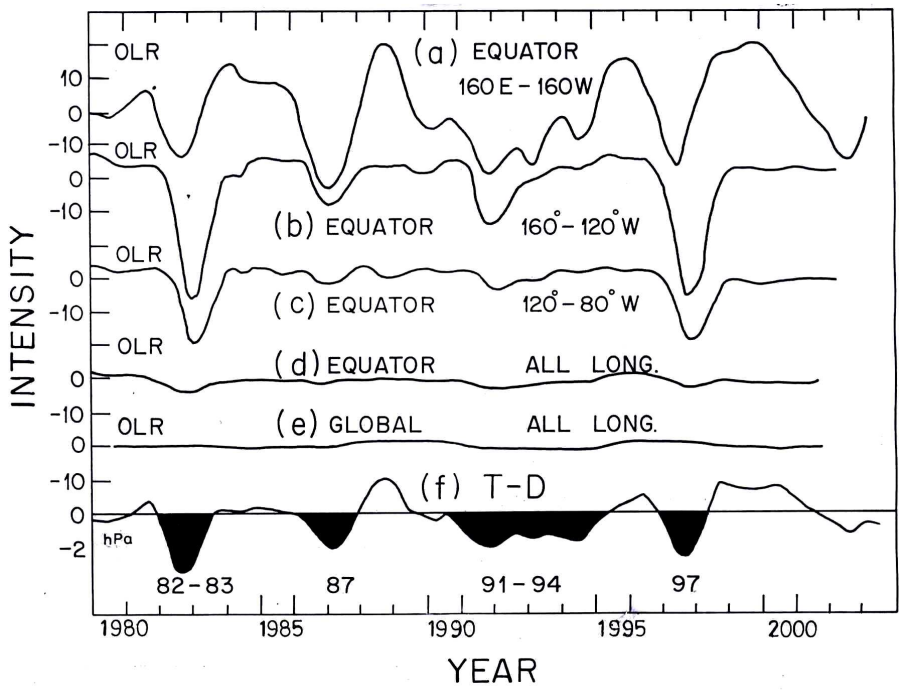

Figs. 1(a-f). Plots of 12-month running means of OLR for equatorial 5° N - 5° S longitudinal belts (a) 160° E - 160° W in the far western Pacific, (b) 160° W - 120° W in the middle Pacific, (c) 120° W - 80° W in the eastern Pacific, (d) all longitudes on the equator and (e) global OLR (all longitudes and latitudes), all on similar scales. Plot (f) is for (T-D), and ENSO (El Niño/Southern Oscillation) index commonly used, namely, Tahiti (T) minus Darwin (D) atmospheric pressure difference (depressions during El Niño events shown black)

central and eastern Sahara and the Arabian Peninsula. The regions of large OLR variance (>10 Wm^{-2}) are over a broad region of the Indian and Pacific Oceans with largest values (>20 Wm^{-2}), on and slightly to the south of the equator in the western Pacific. Further, Warm equatorial Pacific SST anomalies are associated with below normal OLR (enhanced deep atmospheric convection) between 165° E and the Ecuador coast in the equatorial Pacific, and enhanced OLR (diminished convective rainfall) over Papua New Guinea and eastern equatorial Brazil. Thus, OLR patterns different at different geographical locations. However, if global values are calculated, the OLR changes from year to year, or from sunspot maximum to sunspot minimum, are very small (as will be shown further). Thus, climate variability due to OLR on a global scale would be very small as compared to that on regional or sub-regional scales.

In the present communication, the long-term variations of OLR in the equatorial belt are examined for 1974 onwards up to date and compared with those of OLR fluctuations in larger regions.

2. The OLR data were obtained from the website http://www.cpc.ncep.noaa.gov/data/ indices of the Climate Prediction Center, Maryland, USA for the equatorial region in 160° E - 160° W longitudes (20° around the dateline 180°), and from the website http://tao.atmos.washin ton.edu/data sets/olr/index.html for larger regions.

3. Figs. 1 (a-f) shows plots of the 12-month running means of the equatorial OLR (5° N - 5° S) for Longitude belts (a) 160° E - 160° W in the far western Pacific, (b) 160° W - 120° W in the middle Pacific, (c) 120° W - 80° W in the eastern Pacific, (d) all longitudes on the equator and (e) global OLR (all longitudes and latitudes), all on similar scales. Plot (f) is for (T-D), an ENSO (El Niño/Southern Oscillation) index commonly used, namely, Tahiti (T) minus Darwin (D) atmospheric pressure difference. The following may be noted :

In the Pacific, the (T-D) index shows several major depressions (shown black), in 1982-83, 1987, 1991-94, and in 1997-98. These are major El Niño events when positive SST anomalies develop in the Peru-Ecuador coast in S. America and westward in the Pacific. All these El Niños are associated with OLR depressions, but the OLR depressions are largest in the middle Pacific

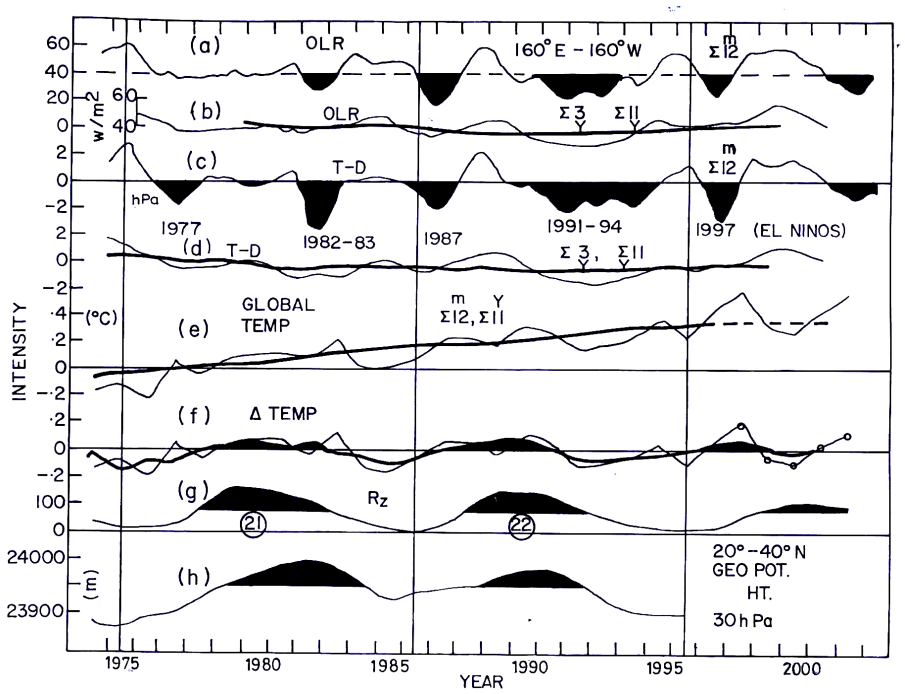

Figs. 2(a-h). Plots of (a) 12-month running means of OLR, (b) 3-year (full line) and 11-year (superposed thick line) moving averages of OLR, (c) 12-month moving averages of T-D, Southern Oscillation Index Tahiti minus Darwin atmospheric pressure difference, (d) 3-year (full line) and 11-year (superposed thick line) moving averages of T-D, (e) annual values (full line) and 11-year moving averages (superposed thick line) of global surface temperatures, (f) de-trended global surface temperature deviations, (g) annual sunspot number Rz, and (h) zonally averaged three-year moving averages of geopotential heights of 30 hPa level for 20° - 40° N

(b) 160° W - 120° W. The average OLR for the equatorial region (d) all longitudes, has comparatively very small year-to-year variations. The global average (all longitudes and latitudes) has negligible year-to-year variations, indicating that global OLR will not be responsible for any major global climatic fluctuations (cloud-radiation/water vapour radiation feedback).

Fig. 2(a) shows the plot of 12-month moving averages of equatorial OLR in the 160° E – 160° W longitude belt, (±20° about the dateline 180°). Large fluctuations are seen which imply that the energy budget in this sub-region of the Earth would vary considerably from year-to-year mainly due to OLR changes due to varying cloud effects. To eliminate the short-term fluctuations, moving averages were calculated over 36 months (3 years). These are shown in Fig. 2(b) as full lines. Here, the effect of the big deviations still remains. The fluctuations are not related to the sunspot cycle (vertical lines mark sunspot minima). To eliminate solar cycle effect also if any, moving averages were calculated over 132 months (11 years). These are shown as the superposed thick line in Fig. 1(b). The long-term OLR level in this sub-region seems to have decreased from 1980 to 1990 by ~15% and then recovered by 2000.

The 12-month running means of the ENSO index (T-D) are plotted in Fig. 2(c) their 3-year and 11-year running means are shown in Fig. 2(d). Here again, there is no relationship with sunspot cycle, and the overall level seems to have decreased from 1980 to 1990 by ~0.6 hPa and then recouped by 2000. This long-term variation is similar for OLR and (T-D), again indicating that the OLR changes in this limited region are mainly due to ENSO activity, on intermediate and long-term time scales also.

The sunspot relationship of terrestrial parameters is somewhat obscure. In spectral analyses, an 11-year signal is often found, but generally, it is not the most prominent periodicity. A parameter intimately related to climate is the global surface temperature. Fig. 2(e) shows a plot of the annual values (full lines) of global surface air temperatures (Jones *et al.*, 1999) and their 11-year moving averages (superposed thick line). The thick line indicates a monotonic temperature increase, generally attributed to green house effects due to increasing carbon dioxide concentration in the atmosphere. If these values are subtracted from the annual values, the residues Δ TEMP are as shown in Fig. 2(f). Compared to the annual sunspot number Rz shown Fig. 2(g), the temperature residues in Fig. 2(f) do show a sunspot cycle association, with a

temperature increase of ~0.2° from sunspot minimum to sunspot maximum, which is gratifying.

Among the various terrestrial parameters, one shows a solar cycle variation clearly, namely, the geopotential height of the lower half of the stratosphere (30 hPa) in the latitude zone 20° - 40° N (vanLoon and Shea, 1999). The plot of 3-year moving averages of annual values is shown in Fig. 2(h). It is surmised by those authors that this sunspot cycle variation is related to a similar variation in tropospheric temperatures.

4. The TSI (Total Solar Irradiance) has only a 0.1% variation during a sunspot cycle. The global OLR also varies very little from year-to-year or during a sunspot cycle. Hence these cannot be responsible for any major climatic changes through the cloud-radiation/water vapour radiation feedback mechanism. However, in smaller regions and sub-regions, OLR fluctuations and related cloudiness fluctuations can be large and can cause large year-to-year climatic fluctuations, notably in the equatorial Pacific region, where El Niño events are very effective.

It must be remembered that TSI is certainly the main external input for terrestrial energy. Hence at least on a longer time scale, TSI should be related to long-term changes of terrestrial parameters. High precision measurements of TSI have been carried out routinely from spacecraft since the 1980s (Willson and Hudson, 1991) and have led to the estimate of 0.1% of variation in phase with sunspot cycle (Reid, 1999). Foukal and Lean (1990) constructed a model of TSI variation between 1874 and 1988 and predicted variations less than 0.1% but noted that additional long-term irradiance changes might be present that could not be detected by the short time period satellite data. Analysing the variability of ionized Ca emissions, Lean *et al.* (1992) concluded that TSI during the seventeenth century Maunder Minimum may have been reduced by 0.24% relative to the present day mean. Nesme-Ribes and Manganey (1992) used observations related to the solar convection zone dynamics and deduced TSI during the Maunder Minimum about 0.5% lower than the current value. Hoyt and Schatten (1993) examined several different solar indices measured over the past centuries and obtained a composite TSI model. From that, Lean *et al*. (1995) calculated solar total and UV irradiances annually from 1610 to 1994 and found that the correlation with northern hemisphere surface temperature was +0.86 in the pre-industrial period 1610-1800, indicating a predominant solar influence. For further period, solar forcing seemed to have contributed about half of the 0.55° C surface warming since 1860 and one third of the warming since 1970, the rest being probably a greenhouse effect due to increase of trace gases (CO_2 etc.). Reid (1997) assumed that the Maunder Minimum temperature was about 1° C lower than today's value and that this required a solar constant (TSI) about 0.6% lower than today's value, and solar forcing could have produced about one-half of the 20th century warming. Thus, different approaches yield different estimates (from 0.05% to 0.60% below the present day level) of the Maunder Minimum TSI, not a satisfactory situation.

5. This work was partially supported by FNDCT, Brazil, under contract FINEP-537/CT.

References

Donnelly, R. F., Hinteregger, H. E. and Sheath, D. F., 1986, "Temporal variations of solar EUIVV, UV and 10,830 - Å radiations", *J. Geophys. Res*., **91**, 5567-5578.

Foukal, P. and Lean, J., 1990, "An empirical model of total solar irradiance variation between 1874 and 1988", *Science*, **247**, 556-558.

Hoyt, D. V. and Schatten, K. H., 1993, "A discussion of plausible solar irradiance variations, 1700-1992", *J. Geophys. Res*., **98**, 18895-18906.

Jones, P. D., New, M., Parker, D. E., Martin, S. and Rigor, I. G., 1999, "Surface air temperature and its changes over the past 150 years", *Rev. Geophys*., **37**, 173-199.

Lean, J., Livingston, W., Skumanich, A. and White, O., 1992, "Estimating the suns's radiative output during the Maunder Minimum", *Geophys. Res. Lett*., **19**, 1591-1594.

Lean, J., Beer, J. and Bradley, R. S., 1995, "Reconstruction of solar irradiance since 1610 : Implications for climatic change", *Geophys. Res. Lett*., **22**, 3195-3198.

Nesme-Ribes, E. and Manganey, A., 1992, "On a plausible physical mechanism connecting the Maunder minimum to the Little Ice Age", *Radiocarbon*, **34**, 263-270.

Reid, G. C., 1997, "Solar forcing of global climate change since the mid-17th century", *Clim. Change*, **37**, 391-405.

Reid, G. C., 1999, "Solar variability and its implications for the human environment", *J. Atmos. Solar-Terr. Phys*., **61**, 3-14.

vanLoon, H. and Shea, D. J., 1999, "A probable signal of the 11-year solar cycle in the troposphere of the Northern Hemisphere", *Geophys. Res. Lett*., **26**, 2893-2896.

Willson, R. C. and Hudson, H. S., 1991, "The sun's luminosity over a complete solar cycle", *Nature*, **351**, 42-44.

R. P. KANE

Instituto Nacional de Pesquisas Espaciais -INPE
C. P. 515, 12245-970-São José dos Campos, SP, BRAZIL
(*2 September 2003, Modified 19 May 2004*)